Bioorg. Med. Chem. 40 (2021) 116194

Contents lists available at ScienceDirect

Bioorganic & Medicinal Chemistry

journal homepage: www.elsevier.com/locate/bmc

Design and synthesis of garlic-related unsymmetrical thiosulfonates as potential Alzheimer's disease therapeutics: *In vitro* and *in silico* study

Kani Zilbeyaz [a,*], Aykut Oztekin [b], Emine Gunbatar Kutluana [a]

[a] Department of Chemistry, Agri Ibrahim Cecen University, Agri, Turkey
[b] Department of Medical Services and Techniques, Agri Ibrahim Cecen University, Agri, Turkey

ARTICLE INFO

Keywords:
Acetylcholinesterase
Butyrylcholinesterase
Enzyme inhibition
Garlic
Organosulfur compounds
Thiosulfonate

ABSTRACT

Garlic contains a wide range of organosulfur compounds, which exhibit a broad spectrum of biological activities. Amongst the sulfur-containing compounds in garlic, the thiosulfonates are considerably popular in various fields. In light of this, we decided to investigate the enzyme inhibition ability of thiosulfonates. In this paper, the synthesis and biological activity of a small library of unsymmetrical thiosulfonates as inhibitors of acetylcholinesterase (AChE) and butyrylcholinesterase (BChE) are described. The activity evaluation revealed nanomolar IC_{50} and K_i values against both enzymes tested. Furthermore, molecular docking studies allowed for the determination of possible binding interactions between the thiosulfonates and AChE.

1. Introduction

Garlic (*Allium sativum* L.) is globally consumed as a food and has been used as a traditional medicine for many centuries. It is superabundant in organosulfur compounds that possess many interesting biological activities including antibacterial,[1] antifungal,[2] antiviral,[3] antiparasitic,[4] anti-inflammatory,[5] antithrombotic,[6] antihypertensive,[7] antioxidant,[8] antiatherosclerotic,[9] and anticarcinogenic.[10–12] Some of the biologically active compounds isolated from garlic are shown in Fig. 1.

These compounds have been extensively studied and each compound is reported to possess more than one pharmacological activity, representative examples are given in Table 1[13] . However, many of these compounds are rapidly transformed into other organosulfur compounds under various conditions. Propyl-propane thiosulfonate is one example of a stable secondary compound from garlic, it is formed by the decomposition of the primary sulfur-containing constituents naturally present in the bulb and is proven to be biologically active.[14–17]

Over the past two decades due to their stability the interest in thiosulfonates as therapeutics has rapidly increased. Thiosulfonates reported to date have been shown to possess anticancer,[18–21] antiparasitic,[22] and antifungal properties,[23] however, to the best of our knowledge, the cholinesterase inhibition properties of thiosulfonates remains unexplored. In light of this and given that the search for new small molecules as potential inhibitors of the cholinesterases has become a topic of interest due to their association with Alzheimer's disease (AD) it was decided to synthesize and screen a small library of thiosulfonates against two cholinesterase enzymes, namely acetylcholinesterase (AChE) and butyrylcholinesterase (BChE).

AD is an irreversible, progressive neurodegenerative disorder that slowly eradicates memory. The principle cause of AD according to the cholinergic hypothesis is a decline in the levels of acetylcholine (ACh), which is hydrolytically degraded by two cholinesterases namely AChE and BChE.[24,25] These cholinesterases are therefore key therapeutic targets for AD. Inhibition of these enzymes by cholinesterase inhibitors (ChEIs) result in higher concentrations of ACh and thus temporary improving the symptoms of AD.[26,27] Unfortunately, there is no cure for AD, the current treatments have unfavorable side effects and the therapeutic strategies are not permanent solutions.[28,29] AD is a serious medical problem and therefore developing new drugs targeting this disease continues to attract interest. Screening various functional scaffolds is a good starting point to scan for potential new lead compounds and thus we report the synthesis and screening results of a library of thiosulfonates as ChEIs. Furthermore, molecular docking studies were undertaken to model the interaction between the thiosulfonates and the enzyme (only AChE was investigated) in order to characterize the behavior of the thiosulfonates in the enzyme binding site.

* Corresponding author at: Agri Ibrahim Cecen University, Faculty of Art and Science, Department of Chemistry, Agri 04100, Turkey.
E-mail address: kbeyaz25@yahoo.com (K. Zilbeyaz).

https://doi.org/10.1016/j.bmc.2021.116194
Received 17 March 2021; Received in revised form 23 April 2021; Accepted 26 April 2021
Available online 1 May 2021

2. Results and discussion

2.1. Synthesis of thiosulfonate derivatives 3–12

A library of unsymmetrical thiosulfonates was prepared by keeping the *p*-tolylsulfonyl group constant and varying the substituent (R group) on the benzyl group attached to the sulfur (II) atom. The various R groups were chosen to address the influence of both the electronic and steric effects on the enzyme inhibition study. The unsymmetrical thiosulfonate derivatives **3**–**12** were synthesized from potassium *p*-toluenethiosulfonate and various substituted benzyl halides in DMF at room temperature for 3 h as outlined in Scheme 1.[30] Compounds **3**–**12** were obtained in good yields (%) and characterized by infrared (IR), high resolution mass spectrometry (HRMS), proton and carbon nuclear magnetic resonance (^{1}H and ^{13}C NMR) spectroscopy.

The ^{1}H and ^{13}C NMR spectra displayed the correct number of resonances as expected for each thiosulfonate derivative **3**–**12**. In the ^{1}H NMR spectra, the presence of the benzylic CH_2 protons of each compound in the series was confirmed by a singlet signal observed in the range δ 4.19–4.32 ppm. In agreement with this the benzylic CH_2 carbon for each compound resonated in the range δ 38.7–40.4 ppm in the ^{13}C NMR spectra. Furthermore, the correct number of proton signals for the benzene rings were observed in the aromatic region in the ^{1}H and ^{13}C NMR spectra.

2.2. Inhibition assay

The synthesized unsymmetrical thiosulfonate compounds **3**–**12** were evaluated as potential inhibitors of human AChE and BChE using a modified version of the Ellman method.[31] To determine the influence of the various substituents at the *para* position of the benzyl ring on the potency of the compounds a structure–activity analysis was performed. The study revealed that the compounds exhibited good inhibitory potential against the enzymes, as evident from their half maximal inhibitory concentration (IC_{50} values) and inhibitory constants (K_i values). Rivastigmine, a clinically used cholinesterase inhibitor, was included in the study for comparison purposes. The IC_{50} and K_i values for each of the target compounds are summarized in Table 2 and Table 3. The results indicated that the potency of the unsymmetrical thiosulfonates **3**–**12** is varied but pleasingly all the compounds inhibited both AChE and BChE in the nanomolar range.

Table 1
Biological activities of a few compounds isolated from garlic.

Compound	Activities
Alliin	Anticancer, Antioxidant, Antidiabetic
Allicin	Antibacterial, Antiviral, Antiprotozoal, Anticancer, Immunomodulatory, Antioxidant, Anti-inflammatory, Antidiabetic
Ajoene	Antiprotozoal, Anticancer, Anti-obesity
Diallyl Sulfide	Anticancer, Antioxidant, Anti-inflammatory
Diallyl Disulfide	Antifungal, Anticancer, Antioxidant
Diallyl Trisulfide	Antiviral, Antifungal, Antiprotozoal, Antioxidant

2.3. Inhibition of AChE

The inhibition of AChE was assessed for **3**–**12** and the results are reported in Table 2. The various electron donating (ED, R = OCH_3, *i*-Pr, *t*-Bu) and electron withdrawing (EW, R = F, Cl, NO_2, CN, CF_3, OCF_3) groups attached to the benzyl ring of compounds **3**–**12** had different effects on the inhibition of AChE. The compounds displayed IC_{50} values ranging from 11.9 nM to 488.2 nM and K_i values ranging from 25.6 ± 2.7 nM to 714.4 ± 82.5 nM. The decreasing order of AChE inhibition by the thiosulfonates according to IC_{50} values is as follow: **11** (*i*-Pr) > **8** (CF_3) > **9** (OCF_3) > **12** (*t*-Bu) > **7** (CN) > **6** (NO_2) > **4** (F) > **5** (Cl) > **10** (OCH_3) > **3** (H). Compound **11** with an ED alkyl group (R = *i*-Pr) showed the most potent inhibitory activity (IC_{50} = 11.9 nM and K_i = 25.6 ± 2.7 nM) amongst the library of thiosulfonates. Comparing **11** with **12** we observe that the activity (IC_{50} = 176.6 nM and K_i = 157.3 ± 28.5 nM for **12**) of the inhibitor decreases as the ED alkyl substituent (R = *t*-Bu) becomes more bulky. The weakest inhibitors in the series according to its IC_{50} values were identified as the parent thiosulfonate **3** (R = H, IC_{50} = 517.4 nM) and **10** (IC_{50} = 667.6 nM) with a methoxy R group. Replacing the methoxy group with a trifluoromethoxy group as in compound **9** (IC_{50} = 129.4 nM) resulted in a fivefold improvement in the inhibition potential. The same effect is observed when comparing **3** (R = H, IC_{50} = 517.4 nM) and **4** (R = F, IC_{50} = 312.5 nM), the fluorine substituent resulted in a 1.7 times better inhibitory activity compared to a hydrogen substituent.

Considering the compounds that contain fluorine atoms (**4** vs **8** vs **9**) it is observed that **8** (R = CF_3, IC_{50} = 86.6 nM) is the more effective inhibitor and the second most potent among the series. Many reports have shown that the presence of fluorine atoms in biologically active molecules can dramatically improve their pharmacological effect.[32,33] Three main reasons have been reported for introducing fluorine atoms

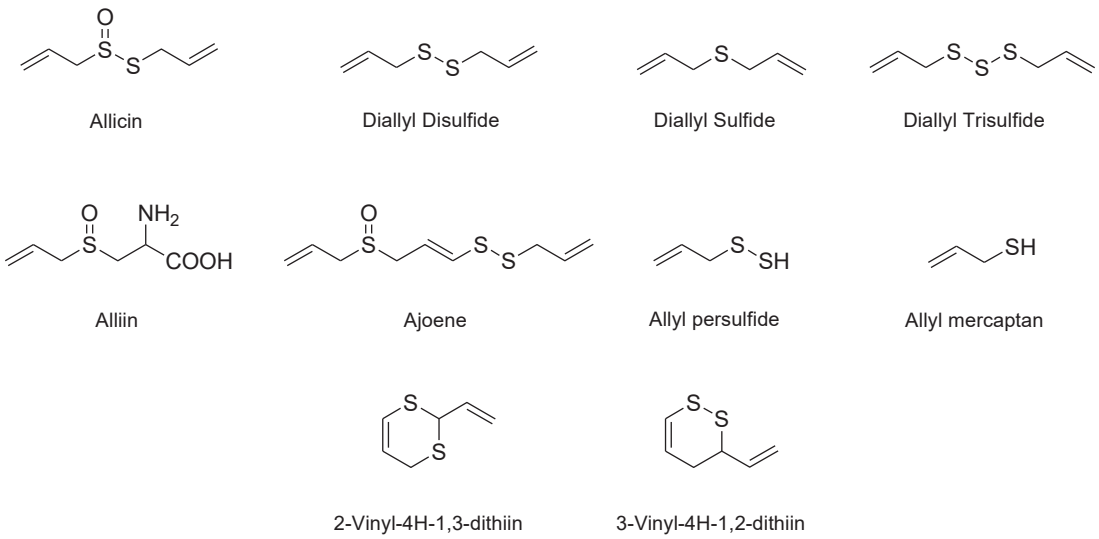

Fig. 1. Chemical structures of a few biological active compounds isolated from garlic.

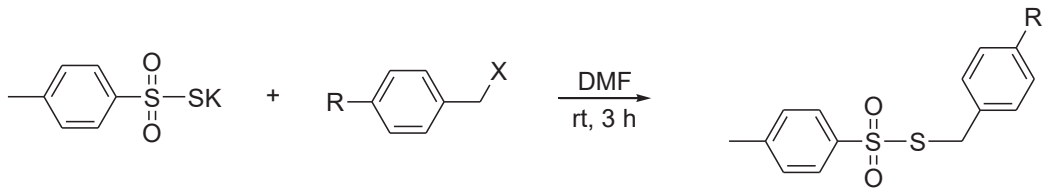

1 2 3-12

Scheme 1. Synthesis of unsymmetrical thiosulfonates **3**–**12** (X = Cl or Br; R = **3**: H, **4**: F, **5**: Cl, **6**: NO_2, **7**: CN , **8**: CF_3, **9**: OCF_3, **10**: OCH_3, **11**: *i*-Pr, **12**: *t*-Bu).

Table 2
Inhibition of AChE by **3**–**12** and standard compound rivastigmine.

Compound	R	IC_{50} (nM)	r^2	K_i (nM)
3	H	517.4	0.94	389.7 ± 62.8
4	F	312.5	0.98	326.9 ± 22.8
5	Cl	478.2	0.93	714.4 ± 82.5
6	NO_2	212.3	0.97	251.4 ± 30.2
7	CN	195.7	0.98	165.5 ± 11.3
8	CF_3	86.6	0.94	147.9 ± 27.5
9	OCF_3	129.4	0.95	198.2 ± 33.0
10	OCH_3	488.2	0.95	218.7 ± 27.67
11	i-Pr	11.9	0.97	25.6 ± 2.7
12	t-Bu	176.6	0.99	157.3 ± 28.5
Rivastigmine		60.0	0.98	–

Table 3
Inhibition of BChE by **3**–**12** and standard compound rivastigmine.

Compound	R	IC_{50} (nM)	r^2	K_i (nM)
3	H	318.5	0.95	217.6 ± 25.6
4	F	302.7	0.93	207.6 ± 9.7
5	Cl	314.5	0.98	198.7 ± 21.8
6	NO_2	214.3	0.97	302.5 ± 51.4
7	CN	202.5	0.96	201.2 ± 31.6
8	CF_3	117.9	0.96	102.6 ± 12.7
9	OCF_3	53.3	0.95	17.5 ± 1.0
10	OCH_3	201.5	0.96	251.5 ± 17.3
11	i-Pr	84.5	0.96	37.9 ± 2.8
12	t-Bu	159.4	0.98	102.1 ± 19.3
Rivastigmine		14.3	0.99	–

into molecules: (i) for improving metabolic stability, (ii) for altering physicochemical properties and (iii) for increasing binding affinity.[32] In light of this, it is not surprising that the fluorinated thiosulfonates were better inhibitors compared to their protonated counterparts. The remaining thiosulfonates, namely **5** (R = Cl, IC_{50} = 478.2 nM), **6** (R = NO_2, IC_{50} = 212.3 nM) and **7** (R = CN, IC_{50} = 195.7 nM) were all more active compared with the parent thiosulfonate **3** (R = H, IC_{50} = 517.4 nM), indicating that the presence of a *para* functional group generally increases the inhibition potential of the compounds. As a final point, it should be noted that besides being the most effective inhibitor, **11** was the only compound more active than the clinically approved reference drug rivastigmine (IC_{50} = 60.0 nM), showing a fivefold improvement compared with the standard.

2.4. Inhibition of BChE

The screening of **3**–**12** against BChE showed that the enzyme was inhibited by all the compounds with IC_{50} and K_i values ranging from 53.3 to 318.5 nM and 17.5 ± 1.0–302.5 ± 51.4 nM, respectively. As for AChE the various *para* substituents on the benzyl ring presented similar trends in the inhibition activity against BChE. The results are shown in Table 3. The decreasing order of BChE inhibition by the thiosulfonates according to the IC_{50} values is as follow: **9** (OCF_3) > **11** (*i*-Pr) > **8** (CF_3) > **12** (*t*-Bu) > **10** (OCH_3) > **7** (CN) > **6** (NO_2) > **4** (F) > **5** (Cl) > **3** (H). In

Table 4
Binding interaction data for **3–12** docked into the active site gorge of AChE.

Compound	[1]ΔG (kcal/mol)	[2]ΔG (kcal/mol)	Estimated K_i (nM)	Experimental K_i (nM)	[3]Interacted Amino Acid Residues	Compound	[1]ΔG (kcal/mol)	[2]ΔG (kcal/mol)	Estimated K_i (nM)	Experimental K_i (nM)	[3]Interacted Amino Acid Residues
3	−8.1	−8.14	1090	389.7 ± 62.8	Tyr 341, Tyr 72, Trp 286	8	−9.2	−8.42	677	147.9 ± 27.5	Phe 295, Trp 286, Leu 289, Tyr 341, Phe 338
4	−8.5	−7.80	1920	326.9 ± 22.8	Phe 338, Phe 297, Tyr 341, Tyr 72, Trp 286	9	−8.7	−7.64	2510	198.2 ± 33.0	Trp 286, Phe 297, Tyr 337, Tyr 124, Gly 448, Trp 86, Glu 202, His 447, Tyr 341
5	−8.5	−7.94	1500	714.4 ± 82.5	Tyr 341, Trp 286, Tyr 72	10	−8.1	−8.35	764	247.9 ± 16.7	Trp 286, Phe 297, Phe 338, Tyr 341, Tyr 72
6	−8.9	−8.15	1050	251.4 ± 30.2	Phe 297, Phe 338, Tyr 341, Tyr 72, Ser 293, Trp 286	11	−9.4	−9.60	92	25.6 ± 2.7	Trp 86, Tyr 337, Tyr 341, Trp 286, Tyr 124, Phe 338, Phe 297, Tyr 72
7	−8.9	−8.12	1110	165.5 ± 11.3	Ser 293, Phe 297, Trp 286, Tyr 72, Tyr 341	12	−9.5	−9.44	120	157.3 ± 28.5	Trp 86, Trp 286, Tyr 72, Tyr 341, Phe 297, Phe 338, Phe 295, Tyr 337

[1] Obtained by the AutoDock 4.2 program.
[2] Obtained by the AutoDock Vina program.
[3] Amino acid residues with Van der Waals interactions are not shown.

this case, all the compounds in the series were better inhibitors than the parent thiosulfonate **3** (IC_{50} = 318.5 nM), the compound with the unsubstituted benzyl ring, making **1** the weakest inhibitor in the library. Addition of hydrophobic EW halogen substituents slightly improved the inhibition activity, **4** (R = F, IC_{50} = 302.7 nM) and **5** (R = Cl, IC_{50} = 314.5 nM). Adding strong EW groups such as nitro (**6**, IC_{50} = 214.3 nM) and cyano (**7**, IC_{50} = 202.5 nM) further enhanced the inhibition activity. Once again, the decrease in inhibition activity going from **11** (IC_{50} = 84.5 nM and K_i = 37.9 ± 2.8 nM) to **12** (IC_{50} = 159.4 nM and K_i = 102.1 ± 19.3 nM) demonstrates the steric hindrance effect of the *t*-butyl substituent. Similarly, replacing the hydrogen atoms with fluorine atoms (compare: **3** and **4, 9** and **10**) saw an increase in inhibition potency of the thiosulfonates.

Compound **9** (IC_{50} = 53.3 nM and K_i = 17.5 ± 1.0 nM) with a trifluoromethoxy substituent exhibited the strongest inhibition followed by **11** (R = *i*-Pr) in which the ED character of the isopropyl group possibly plays a big role. Despite the fact that nanomolar range IC_{50} and K_i values were found in this investigation, the unsymmetrical thiosulfonates were less potent compared with rivastigmine. However, these promising results may be useful in the design of potent cholinesterase inhibitors.

The results revealed that generally all the thiosulfonate compounds screened against AChE and BChE showed relatively good inhibition activity. Four of the thiosulfonates (**6**, **7**, **8** and **11**) were better AChE inhibitors, while the remaining six thiosulfonates (**3**, **4**, **5**, **9**, **10** and **12**) were better BChE inhibitors. Although the thiosulfonates, except **11** against AChE, were less potent at inhibiting AChE and BChE compared to rivastigmine, the IC_{50} and K_i values of compounds **8**, **9**, **11** and **12** demonstrate the superior inhibition potency of the thiosulfonates.

2.5. Molecular docking

Molecular docking studies were performed on AChE complexed with the unsymmetrical thiosulfonate compounds **3**–**12** to understand the differences in their inhibition activity, by analyzing the interactions of the thiosulfonates within the enzyme active site. For the computational method, human AChE crystal structures were used and docking calculations were carried out using the programs AutoDock and AutoDock Vina.[34] The most suitable docking poses of the compounds were used to calculate the potential binding energies and their estimated K_i values, which indicated a behaviour in compliance with the experimental data. These results together with the amino acid residues involved in binding are summarized in Table 4. As presented in the table of results, the binding energies of the compounds were in the range −8.1 to −9.5 kcal/mol for AutoDock and −7.64 to −9.60 kcal/mol for AutoDock Vina.

Interactions between the compounds and the binding cavity of AChE included both bonded and non-bonded interactions. Interpretation of the results discloses that the thiosulfonate moiety play a crucial role in enzyme-ligand binding. Generally both sulfur atoms formed π-sulfur interactions while the oxygen atoms of majority of the thiosulfonates formed hydrogen bonds with various amino acid residues. It is noteworthy to mention that four amino acid residues, namely Tyr 341, Trp 286, Phe 338, and Tyr 124, were involved in each of the complexes between the thiosulfonates and AChE. A visualisation of compounds **6**, **7**, **8**, **9**, **11,** and **12** in the active site of AChE from the molecular docking study is presented in Fig. 2 and Fig. 3. Assessment of the docked complexes revealed that thiosulfonates **8** ($\Delta G_{AutoDockVina}$ = −8.42 kcal/mol), **11** ($\Delta G_{AutoDockVina}$ = −9.60 kcal/mol) and **12** ($\Delta G_{AutoDockVina}$ = −9.44 kcal/mol) showed the lowest binding energies and significant interaction patterns. X-ray crystallography studies revealed that AChE consists of two ligand binding sites; a catalytic active site (CAS) and a peripheral anionic site (PAS).[35] The unsymmetrical thiosulfonates bound mainly to PAS as evident from the numerous interactions with amino acid residues (Tyr 72, Tyr 124, Trp 286, and Tyr 341) found around the entrance to the active site gorge, where PAS is located. It has been reported that PAS comprises of Tyr 72, Asp 74, Tyr 124, Trp 286, and Tyr 341 and that

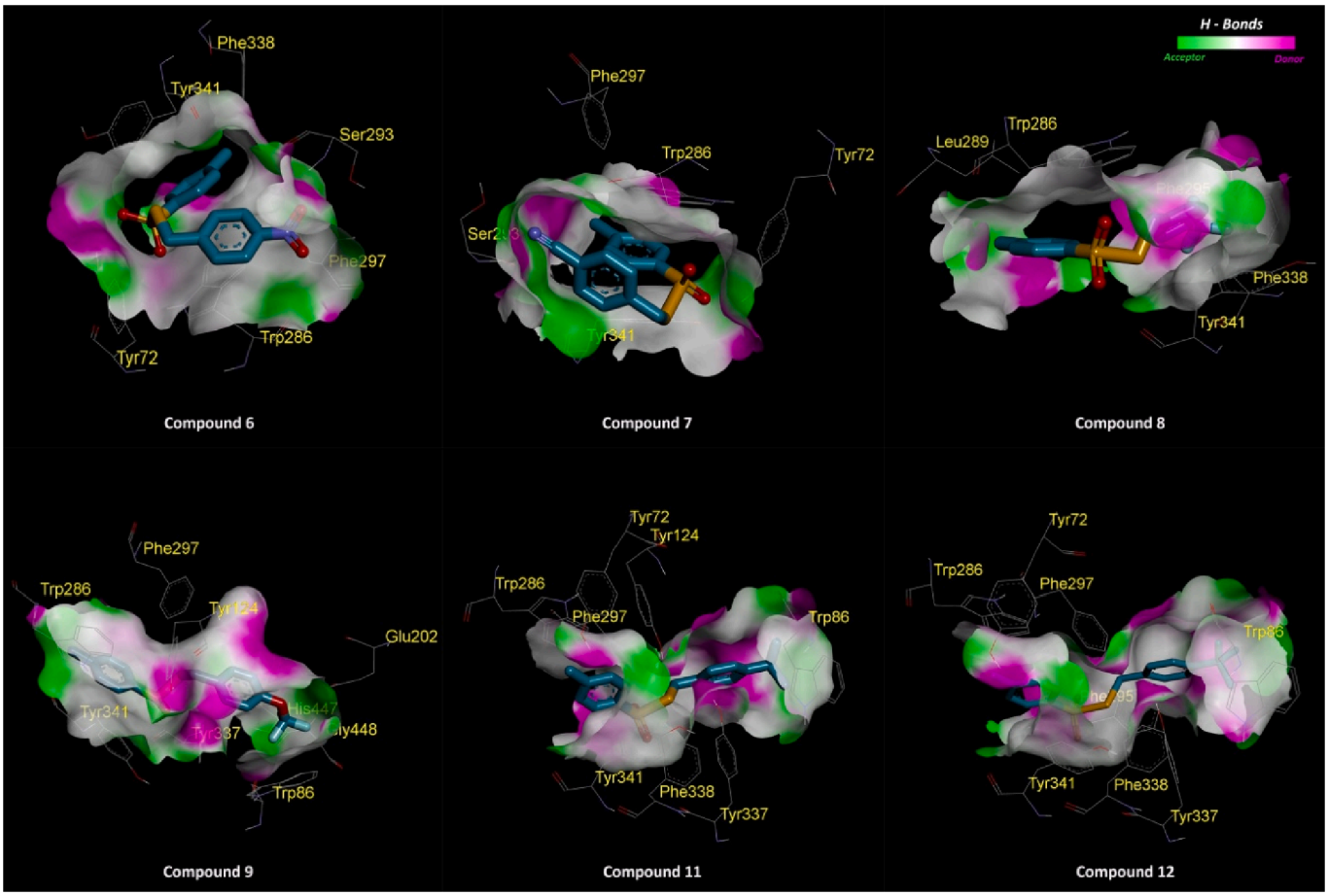

Fig. 2. Binding interactions of **6**, **7**, **8**, **9**, **11**, and **12** with AChE.

inhibitors bound to PAS block the enzyme catalytic activity by limiting substrate traffic.[36–38] The CAS includes a catalytic triad of three amino acids, namely Ser 203, Glu 334, and His 447 at the bottom of the gorge. From the docking results, van de Waals interactions with the amino acid residues (His 447 and Ser 203) in CAS were observed for three ligands, thiosulfonates **9**, **11** and **12**. The results reveal that the thiosulfonate compounds may have potential to be designed as dual binding inhibitors.

Compound **11** displayed the most potent inhibition with a binding energy of −9.6 kcal/mol (AutoDock Vina) and the lowest estimated K_i value (92 nM). These results are in agreement with the *in vitro* studies which also revealed the lowest K_i value for **11** (25.6 ± 2.7 nM) in the series of thiosulfonates tested. The best docked pose of **11** within the active site of AChE is presented in Fig. 4, which shows the interacting amino acid residues of the complex are Trp 86, Tyr 337, Tyr 341, Trp 286, Tyr 124, Phe 338, Phe 297, and Tyr 72. Four of these residues (Trp 86, Tyr 341, Trp 286, and Phe 338) were reported to be crucial targets for designing new AChE inhibitors due to their importance in enzyme catalytic activity.[39] The critical role of these residues is confirmed by the low K_i value obtained for inhibitor **11**.

For compound **11** both the sulfur atoms form π-sulfur interactions with the following amino acids: Tyr 341, Tyr 124, Phe 338 and Phe 297, while the sulfur (II) atom forms a hydrogen bond with the hydroxyl substituent of Try 337. Hydrophobic π-σ interactions were observed between the alkyl groups of the docked thiosulfonate and Trp 86 and Trp 286. The increase in activity observed by **11** and **12** may be attributed to the hydrophobic group attached to the benzyl ring as it has been reported that hydrophobic substituents positively affect inhibition of AChE inhibitors.[40,41] The aromatic moiety forms π-π stacking with Tyr 337, Tyr 341 and Trp 286, which results in stabilization of the complex. In addition, the ligand makes numerous weak Van der Waals interactions with the side chains of various amino acids.

Comparing the binding patterns of the AChE-**11** complex with the AChE-rivastigmine complex (Supplementary Data, Fig. S11) revealed that both compounds form close interactions with important amino acid residues, forming hydrogen bonds, π-σ and Van der Waals interactions, Fig. 4. In the comparison study a few common interactions were observed, these include interactions with the following amino acid residues: Tyr 124, Tyr 72, Trp 86, Tyr 337. Interestingly rivastigmine bound to only one of the important residues (Trp 86) mentioned before, which may explain the five-fold improvement in activity for **11** (IC_{50} = 11.9 nM) compared with the reference standard (IC_{50} = 60.0 nM). Both compounds form π-σ interactions with Trp 86 which is situated in the choline binding site and has been reported to be crucial for inhibition of human AChE.[36] These important enzyme-compound interactions can be exploited to design better inhibitors for AD, which is a destroying lives and haunting society.

Fig. 3. Two-dimensional docking poses of **6**, **7**, **8**, **9**, **11**, and **12** with AChE.

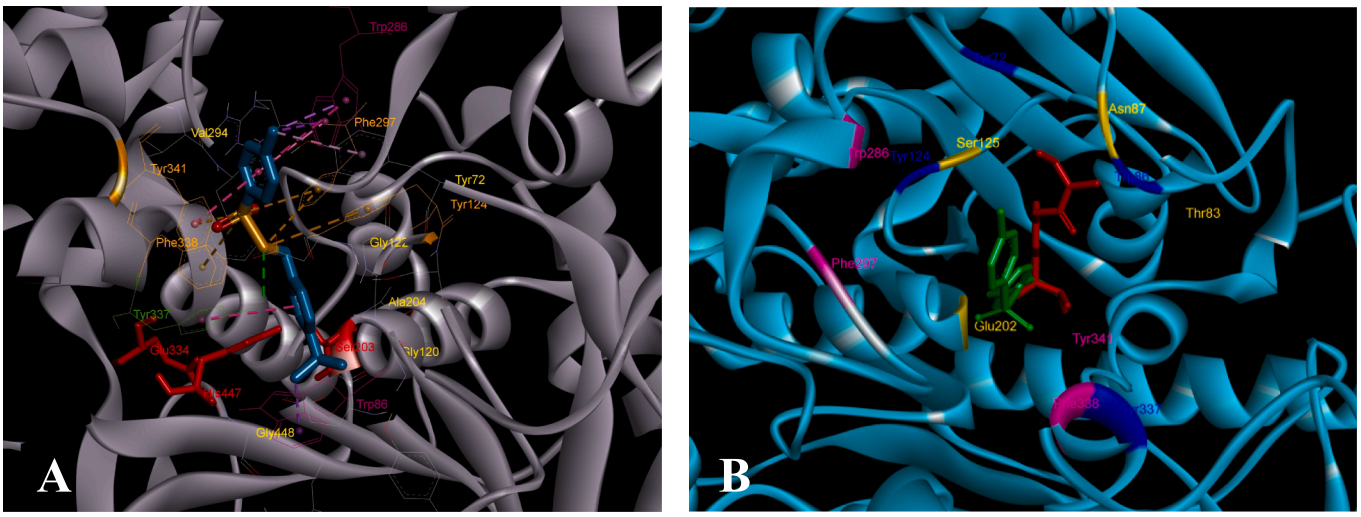

Fig. 4. A: Three-dimensional representation for the interactions of **11** with human AChE. B: Docking of rivastigmine (red) and **11** (green) in the active site of human AChE (the amino acids that interacted with rivastigmine are shown in yellow, with **11** are shown in pink and common interactions are shown in blue).

3. Conclusion

Biological activities of thiosulfonates have been well documented, however, their cholinesterase inhibitory activity has not been reported. In this study, a range of unsymmetrical thiosulfonates were investigated for their effect on AChE and BChE. The screening results revealed nanomolar inhibition rendering the thiosulfonates as potential inhibitors of the enzymes. One candidate, *S*-4-isopropylbenzyl 4-methylbenzenthiosulfonate, presented excellent IC_{50} and K_i values and was more effective than the clinically available ChEI rivastigmine. Molecular docking simulations of *S*-4-isopropylbenzyl 4-methylbenzenthiosulfonate in the active site of AChE provided valuable information regarding the binding interactions of the complex. Overall, these results provide valuable information for the design of potent ChEIs and we trust that *S*-4-isopropylbenzyl 4-methylbenzenthiosulfonate may be a lead candidate for finding new drugs for the treatment of AD.

4. Experimental section

4.1. General procedure: chemicals

All the chemicals and reagents for the synthesis of the unsymmetrical thiosulfonates were purchased from Sigma Aldrich (St. Louis, MO, USA) and used as received without further purification. All solvents were purchased from Merck (Darmstadt, Germany). Thin layer chromatography (TLC) was used to monitor the reactions using aluminium-backed plates coated with silica-gel F_{254}, with visualization using ultra-violet (UV) light. Column chromatography was carried out using silica-gel 60 mesh and petroleum ether:ethyl acetate mixtures as eluent. The unsymmetrical thiosulfonates were stored at −18 °C after they were synthesized. The ^{1}H and ^{13}C NMR spectra were recorded on a Varian Unity 400 spectrometer at 400 MHz for ^{1}H and 100 MHz for ^{13}C using deuteriochloroform ($CDCl_3$) as solvent. All chemical shifts are reported in parts per million (ppm) and all coupling constants are quoted in hertz (Hz). Melting points were measured in open glass capillary tubes on a Stuart SMP30 Melting Point Meter and are uncorrected. Infrared spectra were recorded on a Thermo Nicolet iS10 spectrometer. Electrospray ionization (ESI) mass spectra were recorded using an Agilent 6200 series TOF/6500 series instrument.

4.2. General procedure for the synthesis of compounds 3–12

To a stirred solution of potassium *p*-toluenethiosulfonate (1.3 equiv) dissolved in DMF (1 M) was added dropwise a solution of benzyl halides (1.0 equiv) dissolved in DMF. The solution was allowed to stir at room temperature for 3 h. The reaction was controlled by TLC. After completion the reaction was quenched with saturated aqueous $NaHCO_3$ and the resulting mixture was extracted with CH_2Cl_2 (3 × 15 mL). The combined organic extracts were dried over $MgSO_4$, filtered and the solvent was removed under reduced pressure. The crude residue was purified by silica-gel column chromatography using hexane/ethyl acetate mixtures to afford the desired pure compound.

4.3. S-benzyl 4-methylbenzenthiosulfonate (3)

Obtained as a white solid (75%); m.p. 58–59 °C, lit. m.p. 57–59 °C.[42] IR (cm^{-1}): 3288, 2931, 1590, 1556, 1507, 1418, 1327, 1275, 1139, 1074, 1016, 809, 764, 698, 654. ^{1}H NMR (400 MHz, $CDCl_3$): δ = 2.46 (3H, s, CH_3), 4.27 (2H, s, CH_2), 7.19–7.27 (5H, m, Ar-H), 7.30 (2H, d, J = 8.4 Hz, Ar-H), 7.75 (2H, d, J = 8.4 Hz, Ar-H). ^{13}C NMR (100 MHz, $CDCl_3$): δ = 21.8, 40.4, 127.1, 128.1, 128.9, 129.2, 129.9, 133.8, 142.1, 144.8. HRMS *m/z* (ESI): calculated for $C_{14}H_{18}NO_2S_2$ $[M+NH_4]^+$: 296.0773; found: 296.0763.

4.4. S-4-fluorobenzyl 4-methylbenzenthiosulfonate (4)

Obtained as a white solid (73%); m.p. 44–45 °C. IR (cm^{-1}): 3172, 2928, 1594, 1507, 1417, 1317, 1301, 1290, 1223, 1142, 1073, 1015, 837, 813, 755, 688, 649. ^{1}H NMR (400 MHz, $CDCl_3$): δ = 2.40 (3H, s, CH_3), 4.19 (2H, s, CH_2), 6.87 (2H, t, J = 8.4 Hz, Ar-H), 7.12 (2H, t, J = 8.4 Hz, Ar-H), 7.24 (2H, d, J = 8.4 Hz, Ar-H), 7.67 (2H, d, J = 8.4 Hz, Ar-H). ^{13}C NMR (100 MHz, $CDCl_3$): δ = 20.7, 38.7, 114.8 (d, $J_{C\text{-}F}$ = 21.4 Hz), 126.1, 128.9, 129.9 (d, $J_{C\text{-}F}$ = 8.4 Hz), 141.2, 141.2, 143.9, 161.5 (d, $J_{C\text{-}F}$ = 244.9 Hz). HRMS *m/z* (ESI): calculated for $C_{14}H_{17}FNO_2S_2$ $[M+NH_4]^+$: 314.0679; found: 314.0670.

4.5. S-4-chlorobenzyl 4-methylbenzenthiosulfonate (5)

Obtained as a colourless oil (75%). IR (cm^{-1}): 3401, 3062, 3031, 2985, 2931, 1604, 1496, 1450, 1373, 1303, 1211, 1072. ^{1}H NMR (400 MHz, $CDCl_3$): δ = 2.42 (3H, s, CH_3), 4.20 (2H, s, CH_2), 7.06 (2H, d, J = 8.8 Hz, Ar-H), 7.14 (2H, d, J = 8.8 Hz, Ar-H), 7.25 (2H, d, J = 8.0 Hz, Ar-H), 7.67 (2H, d, J = 8.0 Hz, Ar-H). ^{13}C NMR (100 MHz, $CDCl_3$): δ = 21.8, 39.9, 127.1, 128.9, 129.9, 130.6, 132.6, 134.0, 142.0, 144.9. HRMS *m/z* (ESI): calculated for $C_{14}H_{17}ClNO_2S_2$ $[M+NH_4]^+$: 330.0384; found: 330.0377.

4.6. S-4-nitrobenzyl 4-methylbenzenthiosulfonate (6)

Obtained as a white solid (75%); m.p. 118–119 °C lit. m.p. 120 °C.[43] IR (cm^{-1}): 3178, 2939, 1576, 1558, 1447, 1320, 1293, 1139, 1072, 1013, 885, 811, 705. ^{1}H NMR (400 MHz, $CDCl_3$): $\delta = 2.41$ (3H, s, CH_3), 4.32 (2H, s, CH_2), 7.23 (2H, d, $J = 8.4$ Hz, Ar-H), 7.35 (2H, d, $J = 8.4$ Hz, Ar-H), 7.65 (2H, d, $J = 8.4$ Hz, Ar-H), 8.05 (2H, d, $J = 8.4$ Hz, Ar-H). ^{13}C NMR (100 MHz, $CDCl_3$): δ = 21.7, 39.4, 123.9, 127.1, 129.9, 130.0, 141.9, 142.0, 145.3, 147.5. HRMS *m/z* (ESI): calculated for $C_{14}H_{13}NNaO_4S_2$ $[M+Na]^+$: 346.0178; found: 346.0171.

4.7. S-4-cyanobenzyl 4-methylbenzenthiosulfonate (7)

Obtained as a white solid (78%); m.p. 78–79 °C. IR (cm^{-1}): 3566, 3064, 2959, 2239, 1647, 1558, 1457, 1328, 1259, 1136, 1073, 1053, 1018, 810, 742, 701, 668, 651. ^{1}H NMR (400 MHz, $CDCl_3$): $\delta = 2.44$ (3H, s, CH_3), 4.28 (2H, s, CH_2), 7.25 (2H, d, $J = 8.4$ Hz, Ar-H), 7.30 (2H, d, $J = 8.4$ Hz, Ar-H), 7.50 (2H, d, $J = 8.4$ Hz, Ar-H), 7.66 (2H, d, $J = 8.4$ Hz, Ar-H). ^{13}C NMR (100 MHz, $CDCl_3$): $\delta = 21.4$, 39.5, 111.3, 118.2, 126.8, 129.7, 129.7, 132.2, 139.8, 141.6, 145.0. HRMS *m/z* (ESI): calculated for $C_{15}H_{13}NNaO_2S_2$ $[M+Na]^+$: 326.0280; found: 326.0268.

4.8. S-4-(trifluoromethyl) benzyl 4-methylbenzenthiosulfonate (8)

Obtained as a white solid (79%); m.p. 55–56 °C. IR (cm^{-1}): 3243, 2930, 1590, 1507, 1489, 1419, 1316, 1137, 1106, 1065, 1015, 887, 813, 753, 702, 651. ^{1}H NMR (400 MHz, $CDCl_3$): $\delta = 2.32$ (3H, s, CH_3), 4.22 (2H, s, CH_2), 7.19 (2H, d, $J = 8.4$ Hz, Ar-H), 7.28 (2H, d, $J = 8.0$ Hz, Ar-H), 7.43 (2H, d, $J = 8.4$ Hz, Ar-H), 7.61 (2H, d, $J = 8.0$ Hz, Ar-H). ^{13}C NMR (100 MHz, $CDCl_3$): δ = 21.7, 39.8, 124.0 (q, $J_{C\text{-}F}$ = 270.9 Hz), 125.7 (m), 127.0, 129.5, 129.8, 130,0, 138.4, 142.2, 145.0. HRMS *m/z* (ESI): calculated for $C_{15}H_{17}F_3NO_2S_2$ $[M+NH_4]^+$: 364.0647; found: 364.0628.

4.9. S-4-(trifluoromethoxy) benzyl 4-methylbenzenthiosulfonate (9)

Obtained as a colourless oil (74%). IR (cm^{-1}): 3155, 2931, 1594, 1559, 1507, 1457, 1325, 1255, 1211, 1136, 1075, 1018, 810, 701, 650. ^{1}H NMR (400 MHz, $CDCl_3$): $\delta = 2.41$ (3H, s, CH_3), 4.26 (2H, s, CH_2), 7.05 (2H, d, $J = 8.4$ Hz, Ar-H), 7.19–7.24 (4H, m, Ar-H), 7.66 (2H, d, $J = 8.0$ Hz, Ar-H). ^{13}C NMR (100 MHz, $CDCl_3$): $\delta = 21.7$, 39.6, 120.5 (q, $J_{C\text{-}F}$ = 255.5 Hz), 121.3, 127.0, 129.8, 130.6, 133.0, 142.3, 145.0, 148.9. HRMS *m/z* (ESI): calculated for $C_{15}H_{17}F_3NO3S_2$ $[M+NH_4]^+$: 380.0596; found: 380.0589.

4.10. S-4-methoxybenzyl 4-methylbenzenthiosulfonate (10)

Obtained as a white solid (79%); m.p. 59–60 °C. IR (cm^{-1}): 3214, 2936, 1653, 1540, 1507, 1457, 1318, 1247, 1174, 1137, 1075, 808, 747, 701, 649. ^{1}H NMR (400 MHz, $CDCl_3$): $\delta = 2.44$ (3H, s, CH_3), 3.77 (3H, s, OCH_3), 4.21 (2H, s, CH_2), 6.76 (2H, d, $J = 8.8$ Hz, Ar-H), 7.10 (2H, d, $J = 8.8$ Hz, Ar-H), 7.29 (2H, d, $J = 8.2$ Hz, Ar-H), 7.74 (2H, d, $J = 8.2$ Hz, Ar-H). ^{13}C NMR (100 MHz, $CDCl_3$): $\delta = 21.8$, 40.0, 55.4, 114.3, 125.4, 127.1, 129.9, 130.5, 142.2, 144.7, 159.5. HRMS *m/z* (ESI): calculated for $C_{15}H_{20}NO_3S_2$ $[M+NH_4]^+$: 326.0879; found: 326.0860.

4.11. S-4-isopropylbenzyl 4-methylbenzenthiosulfonate (11)

Obtained as a colourless oil (75%). IR (cm^{-1}): 3567, 2961, 1647, 1594, 1457, 1323, 1138, 1076, 1053, 1018, 810, 737, 701, 650, 621. ^{1}H NMR (400 MHz, $CDCl_3$): $\delta = 1.21$ (6H, d, $J = 6.8$ Hz, CH_3), 2.43 (3H, s, CH_3), 2.85 (1H, sep, $J = 6.8$ Hz, CH), 4.24 (2H, s, CH_2), 7.08–7.12 (4H, m, Ar-H), 7.27 (2H, d, $J = 7.8$ Hz, Ar-H), 7.73 (2H, d, $J = 7.8$ Hz, Ar-H). ^{13}C NMR (100 MHz, $CDCl_3$): δ = 21.8, 24.0, 33.9, 40.3, 126.9, 127.1, 129.2, 129.8, 131.0, 142.3, 144.6, 149.0. HRMS *m/z* (ESI): calculated for $C_{17}H_{20}NaO_2S_2$ $[M+Na]^+$: 343.0797; found: 343.0782.

4.12. S-4-tert-butylbenzyl 4-methylbenzenthiosulfonate (12)

Obtained as a white solid (76%); m.p. 65–66 °C. IR (cm^{-1}): 3163, 2952, 1595, 1558, 1472, 1418, 1319, 1138, 1076, 1017, 1015, 837, 807, 728, 753, 702, 651. ^{1}H NMR (400 MHz, $CDCl_3$): $\delta = 1.30$ (9H, s, CH_3), 2.45 (3H, s, CH_3), 4.26 (2H, s, CH_2), 7.13 (2H, d, J = 8.0 Hz, Ar-H), 7.27–7.29 (4H, m, Ar-H), 7.74 (2H, d, J = 8.4 Hz, Ar-H). ^{13}C NMR (100 MHz, $CDCl_3$): δ = 21.8, 31.4, 34.7, 40.1, 125.9, 127.1, 129.0, 129.8, 130.7, 142.3, 144.6, 151.2. HRMS *m/z* (ESI): calculated for $C_{18}H_{22}NaO_2S_2$ $[M+Na]^+$: 357.0953; found: 357.0957.

4.13. Cholinesterase activity assay

The cholinesterase inhibition activities of the unsymmetrical thiosulfonates compounds were measured by the assay described by Ellman and co-workers with some modifications applied.[31] The activity assays were conducted using human serum butyrylcholinesterase (BChE) and recombinant human acetylcholinesterase (AChE). Acetylthiocholine iodide and butyrylthiocholine iodide (both purchased from Sigma-Aldrich, USA) were used as substrates in the reactions catalyzed by AChE and BChE, respectively. Hydrolysis of the substrates by the enzymes leads to the formation of thiocholine, which reacts with 5,5′dithiobis-2-nitrobenzoic acid (DTNB: Ellman's reagent, Sigma-Aldrich) to form the 5-thio-2-nitrobenzoate anion which exhibits maximum absorbance at 412 nm. Briefly, the reaction mixture was prepared in microplate wells and consisted of the test compounds **3–12** (varied concentrations in the range 1–500 nM), 0.1 M of Tris/HCl buffer (pH 8), 25 μM of DTNB and 10 μL of enzyme solution (0.20 units/mL of AChE and 0.22 units/mL of the BChE). The mixture was incubated at 25 °C for 10 min, which was followed by addition of 0.5 mM acetylthiocholine/butyrylthiocholine iodide to start the reaction. The total volume of the reaction mixture added up to 250 μL. Inhibitory activity was determined by measuring the increase in absorbance at 412 nm by a Multiskan™ GO UV/Vis microplate reader (Thermo Fisher Scientific Spectrophotometer). The IC_{50} values were calculated from activity % versus concentrations graphs, while the K_i values were obtained from Lineweaver–Burk graphs (three different concentrations of the compounds and five different concentrations of each substrate). Rivastigmine was used as a reference standard.

4.14. Molecular modeling studies

The 3D crystal structure of human AChE (PDB ID: 4M0E) was used,[44] which was downloaded from the Protein Data Bank (https://www.rcsb.org). The macromolecule preparation protocol for the docking analyses was followed on AutoDockTools 1.5.6. Water molecules were removed, non polar hydrogens were merged and Gasteiger charges were added. The chemical 2D structures of the compounds (**3–12**) were drawn using ChemDraw 19.1. The structures were then transferred to the Avogadro program for optimizing the 3D conformations. After preparation of the ligands and receptor, structural based computational analysis were separately performed with both AutoDock and AutoDock Vina at the PyRx platform.[34] Discovery Studio Visualizer was utilized to analyze and visualize the 3D models of the docked conformations and interactions.[45]

Declaration of Competing Interest

The authors declare that they have no known competing financial interests or personal relationships that could have appeared to influence the work reported in this paper.

Acknowledgements

The authors would like to thank Agri Ibrahim Cecen University Scientific Research Council for funding (Project No: FEF.20.005).

Ethical statement

There is no need to provide ethical approval in terms of content and method of this study.

Appendix A. Supplementary material

Supplementary data to this article can be found online at https://doi.org/10.1016/j.bmc.2021.116194.

References

1 Palaksha MN, Ahmed M, Das S. Antibacterial activity of garlic extract on streptomycin-resistant *Staphylococcus aureus* and *Escherichia coli* solely and in synergism with streptomycin. *J Nat Sci Biol Med*. 2010;1:12–15. https://doi.org/10.4103/0976-9668.71666.

2 Li WR, Shi QS, Dai HQ, et al. Antifungal activity, kinetics and molecular mechanism of action of garlic oil against *Candida albicans*. *Sci Rep*. 2016;6:22805. https://doi.org/10.1038/srep22805.

3 Weber ND, Andersen DO, North JA, Murray BK, Lawson LD, Hughes BG. In vitro virucidal effects of *Allium sativum* (garlic) extract and compounds. *Planta Med*. 1992;58:417–423. https://doi.org/10.1055/s-2006-961504.

4 Soffar SA, Mokhtar GM. Evaluation of the antiparasitic effect of aqueous garlic (*Allium sativum*) extract in *Hymenolepiasis nana* and *Giardiasis*. *J Egyptian Soc Parasitol*. 1991;21:497–502.

5 Lee DY, Li H, Lim HJ, Lee HJ, Jeon R, Ryu J-H. Anti-inflammatory activity of sulfur-containing compounds from garlic. *J Med Food*. 2012;15:992–999. https://doi.org/10.1089/jmf.2012.2275.

6 El-Sabban F. Garlic as an antithrombotic and antiplatelet aggregation agent. *J Chin Clin Med*. 2009;4:288–294.

7 Ried K, Fakler P. Potential of garlic (*Allium sativum*) in lowering high blood pressure: mechanisms of action and clinical relevance. *Integr Blood Press Control*. 2014;7:71–82. https://doi.org/10.2147/IBPC.S51434.

8 Boonpeng S, Siripongvutikorn S, Sae-Wong C, Sutthirak P. The antioxidant and anti-cadmium toxicity properties of garlic extracts. *Food Sci Nutr*. 2014;2:792–801. https://doi.org/10.1002/fsn3.164.

9 Sobenin IA, Andrianova IV, Lakunin KY, Karagodin VP, Bobryshev YV, Orekhov AN. Anti-atherosclerotic effects of garlic preparation in freeze injury model of atherosclerosis in cholesterol-fed rabbits. *Phytomedicine*. 2016;23:1235–1239. https://doi.org/10.1016/j.phymed.2015.10.014.

10 Li S, Yang G, Zhu X, Cheng L, Sun Y, Zhao Z. Combination of rapamycin and garlic-derived S-allylmercaptocysteine induces colon cancer cell apoptosis and suppresses tumor growth in xenograft nude mice through autophagy/p62/Nrf2 pathway. *Oncol Rep*. 2017;38:1637–1644. https://doi.org/10.3892/or.2017.5849.

11 LV Y, So KF, Wong NK, Xiao J. Anti-cancer activities of *S*-allylmercaptocysteine from aged garlic. *Chin J Nat Med*. 2019;17:43–49. https://doi.org/10.1016/S1875-5364(19)30008-1.

12 Rose P, Moore PK, Whiteman M, Zhu Y-Z. An appraisal of developments in Allium Sulfur Chemistry: Expanding the pharmacopeia of Garlic. *Molecules*. 2019;24(21):4006. https://doi.org/10.3390/molecules24214006.

13 Batiha GES, Beshbishy AM, Wasef LG, et al. Chemical constituents and pharmacological activities of garlic (*Allium sativum* L.): a review. *Nutrients*. 2020;12:872. https://doi.org/10.3390/nu12030872.

14 Sorlozano-Puerto A, Albertuz-Crespo M, Lopez-Machado I, et al. In vitro antibacterial activity of propyl-propane-thiosulfinate and propyl-propane-thiosulfonate derived from *Allium* spp. against Gram-Negative and Gram-Positive multidrug-resistant bacteria isolated from human samples. *Biomed Res Int*. 2018;2018, 7861207. https://doi.org/10.1155/2018/7861207.

15 Vezza T, Algieri F, Garrido-Mesa J, et al. The immunomodulatory properties of propyl-propane thiosulfonate contribute to its intestinal anti-inflammatory effect in experimental colitis. *Mol Nutr Food Res*. 2019;63:1800653. https://doi.org/10.1002/mnfr.201800653.

16 Lira AC, Prieto AI, Banos A, et al. Safety assessment of propyl-propane-thiosulfonate (PTSO): 90-days oral subchronic toxicity study in rats. *Food Chem Toxicol*. 2020;144, 111612. https://doi.org/10.1016/j.fct.2020.111612.

17 Sorlozano-Puerto A, Albertuz-Crespo M, Lopez-Machado I, et al. Antibacterial and antifungal activity of propyl-propane-thiosulfinate and propyl-propane-thiosulfonate, two organosulfur compounds from *Allium cepa*. In Vitro antimicrobial effect via the gas phase. *Pharmaceuticals*. 2021;14:21. https://doi.org/10.3390/ph14010021.

18 Smith M, Hunter R, Stellenboom N, et al. They cytotoxicity of garlic-related disulphides and thiosulfonates in WHCO1 oesophageal cancer cancer cells is dependent on *S*-thiolation and not production of ROS. *Biochim Biophys Acta*. 2016;1860:1439–1449. https://doi.org/10.1016/j.bbagen.2016.03.032.

19 Gabriele E, Ricci C, Meneghetti F, Ferri N, Asai A, Sparatore A. Methanethiosulfonate derivatives as ligands of the STAT3-SH2 domain. *J Enzyme Inhib Med Chem*. 2017;32:337–344. https://doi.org/10.1080/14756366.2016.1252757.

20 Lubenets VI, Parashchyn ZD, Vasylyuk SV, Novikov VP. The S-methyl-(2-methoxycarbonylamino-benzimidazole-5) thiosulfonate as a potential anticancer agents. *Global J Pharm Pharm Sci*. 2017;3(2), 555607. https://doi.org/10.19080/GJPPS.2017.03.555607.

21 Khodyuk RGD, Bai R, Hamel E, et al. Diaryl disulfides and thiosulfonates as combretastatin A-4 analogues: Synthesis, cytotoxicity and antitubulin activity. *Bioorg Chem*. 2020;101, 104017. https://doi.org/10.1016/j.bioorg.2020.104017.

22 Dmitryjuk M, Szczotko M, Kubiak K, et al. S-methyl-(2-methoxycarbonylamino-benzimidazole-5) thiosulfonate as a potential antiparasitic agent - Its action on the development of *Ascaris suum* eggs in vitro. *Pharmaceuticals*. 2020;13:332. https://doi.org/10.3390/ph13110332.

23 Baerlocher FJ, Baerlocher MO, Chaulk CL, Langler RF, MacQuarrie SL. Antifungal thiosulfonates: potency with some selectivity. *Aust J Chem*. 2000;53:399–402. https://doi.org/10.1071/CH00030.

24 Nordberg A, Ballard C, Bullock R, Darreh-Shori T, Somogyi M. A review of butyrylcholinesterase as a therapeutic target in the treatment of Alzheimer's disease. *Prim Care Companion CNS Disord*. 2013;15(2). PCC.12r01412.

25 Marucci G, Buccioni M, Ben DD, Lambertucci C, Volpini R, Amenta F. Efficacy of acetylcholinesterase inhibitors in Alzheimer's disease. *Neuropharmacology*. 2020;6, 108352. https://doi.org/10.1016/j.neuropharm.2020.108352.

26 Stellenboom N. Inhibition of carbonic anhydrase, acetylcholinesterase and butyrylcholinesterase by BisPMB, a synthetic analogue of ajoene. *J Turkish Chem Soc*. 2019;6:143–148. https://doi.org/10.18596/jotcsa.484444.

27 Stellenboom N. Comparison of the inhibitory potential towards carbonic anhydrase, acetylcholinesterase and butyrylcholinesterase of chalcone and chalcone epoxide. *J Biochem Mol Toxicol*. 2019;33, e22240. https://doi.org/10.1002/jbt.22240.

28 Weinstock M. Selectivity of cholinesterase inhibition. *CNS Drugs*. 1999;12:307–323.

29 Sharma K. Cholinesterase inhibitors as Alzheimer's therapeutics (Review). *Mol Med Rep*. 2019;20:1479–1487. https://doi.org/10.3892/mmr.2019.10374.

30 Kaschula CH, Hunter R, Stellenboom N, et al. Structure-activity studies on the anti-proliferation activity of ajoene analogues in WHCO1 oesophageal cancer cells. *Eur J Med Chem*. 2012;50:236–254. https://doi.org/10.1016/j.ejmech.2012.01.058.

31 Ellman GL, Courtney KD, Andres V, Featherstone RM. A new and rapid colorimetric determination of acetylcholinesterase activity. *Biochem Pharmacol*. 1961;7:88–90. https://doi.org/10.1016/0006-2952(61)90145-9.

32 Shah P, Westwell AA. The role of fluorine in medicinal chemistry. *J Enzyme Inhib Med Chem*. 2007;22:527–540. https://doi.org/10.1080/14756360701425014.

33 Xing L, Blakemore DC, Narayanan A, et al. Fluorine in drug design: a case study with fluoroanisoles. *Chem Med Chem*. 2015;10:715–726. https://doi.org/10.1002/cmdc.201402555.

34 Trott O, Olson AJ. AutoDock Vina: improving the speed and accuracy of docking with a new scoring function, efficient optimization and multithreading. *J Comput Chem*. 2010;31:455–461. https://doi.org/10.1002/jcc.21334.

35 Cheung J, Rudolph MJ, Burshteyn F, et al. Structures of human acetylcholinesterase in complex with pharmacologically important ligands. *J Med Chem*. 2012;55:10282–10286. https://doi.org/10.1021/jm300871x.

36 Ordentlich A, Barak D, Kronman C, et al. Dissection of the human acetylcholinesterase active center determinants of substrate specificity. Identification of residues constituting the anionic site, the hydrophobic site, and the acyl pocket. *J Biol Chem*. 1993;268:17083–17095.

37 Bourne Y, Radic Z, Sulzenbacher G, Kim E, Taylor P, Marchot P. Substrate and product trafficking through the active center gorge of acetylcholinesterase analyzed by crystallography and equilibrium binding. *J Biol Chem*. 2006;281:29256–29267. https://doi.org/10.1074/jbc.M603018200.

38 Johnson G, Moore SW. The peripheral anionic site of acetylcholinesterase: structures, functions and potential role in rational drug design. *Curr Pharm Des*. 2006;12:217–225. https://doi.org/10.2174/138161206775193127.

39 Damuka N, Kammari K, Potshangbam AM, Rathore RS, Kondapi AK, Vindal V. Discovery of dual cation-π inhibitors of acetylcholinesterase: design, synthesis and biological evaluation. *Pharmacol Rep*. 2020;72:705–718. https://doi.org/10.1007/s43440-020-00086-2.

40 Lin G, Liao WC, Chan CH, Wu YH, Tsai HJ, Hsieh CW. Quantitative structure-activity relationships for the pre-steady state acetylcholinesterase inhibition by carbamates. *J Biochem Mol Toxicol*. 2004;18:353–360. https://doi.org/10.1002/jbt.20045.

41 Imramovsky A, Stepankova S, Vanco J, et al. Acetylcholinesterase-inhibiting activity of salicylanilide *N*-alkylcarbamates and their molecular docking. *Molecules*. 2012;17:10142–10158. https://doi.org/10.3390/molecules170910142.

42 Goodridge RJ, Hambley TW, Haynes RK, Ridley DD. Preparation of stable, camphor-derived, optically active allyl and alkyl sulfoxides and thermal epimerization of the allyl sulfoxides. *J Org Chem*. 1988;53:2881–2889. https://doi.org/10.1021/jo00248a001.

43 Loudon JD, Livingston A. Exchange of sulphonyl groups in thiolsulphonic esters. *J Chem Soc*. 1935;896–898. https://doi.org/10.1039/JR9350000896.

44 Cheung J, Gary EN, Shiomi K, Rosenberry TL. Structures of human acetylcholinesterase bound to dihydrotanshinone I and territrem B show peripheral site flexibility. *ACS Med Chem Lett*. 2013;4:1091–1096. https://doi.org/10.1021/ml400304w.

45 Dassault Systeme BIOVIA, DSME, R, 2017. San Diego: Dassault Systeme; 2016.